Inorg. Chem. **2008**, *47*, 454–467

Routes to New Hafnium(IV) Tetraaryl Porphyrins and Crystal Structures of Unusual Phosphate-, Sulfate-, and Peroxide-Bridged Dimers

Alexander Falber,[†] Louis Todaro,[†] Israel Goldberg,*[,‡] Michael V. Favilla,[†] and Charles Michael Drain*[,†,§]

Hunter College and Graduate Center of the City University of New York, 695 Park Avenue, New York, New York 10065, Tel Aviv University, Ramat Aviv, Israel, and The Rockefeller University, 1230 York Avenue, New York, New York 10065

Received May 1, 2007

New routes for the synthesis of mono tetraaryl porphyrinato hafnium(IV) complexes, Hf(IV)Por$(L)_2$, are reported, where the secondary ligands, L, are determined by the method of purification. These synthetic routes cater to the solubility of the macrocycles and provide access to Hf(IV) complexes of meso tetraaryl porphyrins bearing diverse functional groups such as phenyl, tolyl, pyridyl, pentafluorophenyl, and carboxyphenyl. The latter three derivatives significantly expand the repertoire of hafnium porphyrinates. One route refluxes the porphyrin with $HfCl_4$ in 1-chloronaphthalene or in a mixed solvent of 1-chloronaphthalene and *o*-cresol. A second, solventless method is also reported wherein the porphyrin is mixed with $Hf(cp)_2Cl_2$ and heated to give the metalated porphyrin in good yields. Simultaneous purification and formation of stable porphyrinato hafnium(IV) diacetate complexes, Hf(Por)-OAc_2, is accomplished by elution over silica gel using 3–5% acetic acid in the eluent. Exchange of the acetate ligands for other oxo-bearing ligands can be nearly quantitative, such as *p*-aminobenzoate (PABA), pentanoate (pent), or octanoate (oct). Notably, we find that two to three of a variety of small multitopic dianions such as peroxo (O_2^{-2}), SO_4^{-2}, and HPO_4^{-2} serve to bridge between two Hf(Por) moieties to form stable dimers. The crystal structures of this library of Hf(Por) complexes are reported, and we note that careful analysis of crystallography data reveals (Por)Hf(μ-η^2-O_2)$_2$Hf(Por) rather than four bridging oxo or hydroxy ions.

Introduction

To date, the chemistry of hafnium(IV) porphyrinates[1−17] remains undeveloped, being limited to octaethylporphyrin (OEP) and tetraphenylporphyrin (TPP), with a small variety of derivatives with different anions to balance the remaining 2+ charge and ligands to satisfy the 7−8 coordination sphere. These derivatives have the general formula Hf(Por)L_2[2,8,9,18]

* To whom correspondence should be addressed. (C.M.D) E-mail: cdrain@hunter.cuny.edu. Phone: 212-650-3791. Fax: 212-772-5332. (I.G.): E-mail: goldberg@post.tau.ac.il. Phone: 972-3-6409965. Fax: 972-3-6409293.

† City University of New York.

‡ Tel Aviv University.

§ The Rockefeller University.

(1) Ryu, S.; Whang, D.; Kim, J.; Yeo, W.; Kim, K. *J. Chem. Soc., Dalton Trans.* **1993**, 205−209.
(2) Ryu, S.; Kim, J.; Yeo, H.; Kim, K. *Inorg. Chim. Acta* **1995**, *228*, 233−236.
(3) Afzal, D.; Baughman, R.; James, A.; Westmeyer, M. *Supramol. Chem.* **1996**, *6*, 395−399.
(4) Huhmann, J. L.; Rath, N. P.; Corey, J. Y. *Acta Crystallogr., Sect. C: Cryst. Struct. Commun.* **1996**, *52*, 2486−2488.
(5) Knor, G.; Strasser, A. *Inorg. Chem. Commun.* **2002**, *5*, 993−995.
(6) Tipugina, M. Y.; Lomova, T. N. *Russ. J. Inorg. Chem.* **2004**, *49*, 961−965.
(7) Martin, P. C.; Arnold, J.; Bocian, D. F. *J. Phys. Chem.* **1993**, *97*, 1332−1338.
(8) Brand, H.; Capriotti, J. A.; Arnold, J. *Organometallics* **1994**, *13*, 4469−4473.
(9) Huhmann, L. J.; Corey, J. Y.; Rath, N. P.; Campana, C. F. *J. Organomet. Chem.* **1996**, *513*, 17−26.
(10) Ryu, S.; Whang, D.; Kim, H. J.; Kim, K.; Yoshida, M.; Hashimoto, K.; Tatsumi, K. *Inorg. Chem.* **1997**, *36*, 4607−4609.
(11) Thorman, J. L.; Guzei, I. A.; Young, V. G.; Woo, L. K. *Inorg. Chem.* **1999**, *38*, 3814−3824.
(12) Thorman, J. L.; Guzei, I. A.; Young, V. G.; Woo, K. L. *Inorg. Chem.* **2000**, *39*, 2344−2351.
(13) Tomachynski, L. A.; Chernii, V. Y.; Volkov, S. V. *J. Porphyrins Phthalocyanines* **2001**, *5*, 731−734.
(14) Tomachynski, L. A.; Chernii, V. Y.; Volkov, S. V. *Russ. J. Inorg. Chem.* **2002**, *47*, 208−211.
(15) Gerasymchuk, Y. S.; Chernii, V. Y.; Tomachynski, L. A.; Legendziewicz, J.; Radzki, S. *Opt. Mater.* **2005**, *27*, 1484−1494.
(16) Knor, G.; Strasser, A. *Inorg. Chem. Commun.* **2005**, *8*, 471−473.
(17) (a) Buchler, J. W.; Decian, A.; Fischer, J.; Hammerschmiitt, P.; Weiss, R. *Chem. Ber.* **1991** *124*, 1051−1058. (b) K. M. Kadish, K.; Smith, K. M.; Guilard, R. Eds. *The Porphyrin Handbook*; Academic Press: New York, 2000; Vols. 1−10. (c) Dolphin, D. Ed. *The Porphryins*; Academic Press, 1978; Vols. 1−7. (d) Also suggested by a reviewer.
(18) Du, G.; Woo, L. K. *Organometallics* **2003**, *22*, 450−455.

10.1021/ic700840j CCC: $40.75
Published on Web 12/19/2007

where L = Cl^-, OAc^-, $P_2O_7^-$ and organometallic species CH_3, and *n*-butyl. The reactivity[19] and the previously reported synthetic methods for hafnium(IV) and zirconium(IV) porphyrinates are generally similar and are carried out in refluxing solvents (benzonitrile, dimethoxyethane, or toluene) using the $HfCl_4$ starting complex with 80−95% yields of the M(Por)Cl_2 complex. The metal ions in these complexes are oxophilic; thus, the preference for carboxylate or other oxygen-bearing anionic ligands. In analogy to the zirconium(IV) porphyrinates,[19−30] which also are almost entirely OEP and TPP derivatives, much of the research on Hf(Por)L_2 compounds has centered on the organometallic chemistry[2,18,19,22] and the potential catalytic properties. Zr(IV) has an electron configuration of [Kr], and Hf(IV) has that of [Xe] 4f,[14] so both are closed shell metal ions. Because of the lack of functional groups on the porphyrin moieties, there is a paucity of supramolecular materials with designed, hierarchical structures[31−46] containing Zr(Por) or Hf(Por). Hafnium(IV) porphyrinates, and by analogy the zirconium(IV) porphyrinates, have an excellent potential for constructing robust supramolecular architectures for several reasons: (1) Hf(IV) is strongly ligated by the porphyrin, being resistant to demetalation by acids, bases, and high temperature, (2) the large coordination sphere, ionic radius, and the 4+ charge results in coordination of the hafnium ion outside the plane of the macrocycle and requires auxiliary ligands, (3) both the auxiliary ligands and the porphyrin can bear nitrogenous moieties for self-assembly mediated by metal ions or by hydrogen bonding since Hf is oxophilic. The self-organization of Hf porphyrins into materials[35,47] requires an expanded repertoire of macrocycles with functional groups designed for discrete intermolecular interactions.[31−45,48]

Herein, we focus on routes that result in Hf(IV) chelation by meso tetraaryl porphyrins bearing functional groups that we find are not amenable to previously reported methods and require strategies tailored to macrocycle solubility and reactivity. The complexes bearing pyridyl, carboxyphenyl, and pentaflourophenyl moieties can serve as tectons for the construction of hierarchically structured materials. The methods are amenable to small 50 mg scales as well as 300 mg batches and minimize solvent use in synthesis. A purification strategy is described that simultaneously allows exchange of the initially formed chlorides for oxophilic ligands. These methods take advantage of the oxophilic nature of the Hf(IV) center and use the stable Hf(Por)OAc_2 as a starting point for a variety of other derivatives.

Experimental Procedures

Instrumentation and Reagents. All UV-visible spectra were taken in 1 cm quartz or glass cuvettes in CH_2Cl_2 on a Carey Bio 3 spectrophotometer unless otherwise indicated. Mass spectrometry was done as a service by the University of Illinois, Urbana−Champaign or on an Agilent 1100 LC/MSD instrument. NMR spectra were run on a 500 MHz Varian Inova and chemical shifts (ppm) are referenced to the proton solvents. Fluorescence spectra were taken on a Spex Tau-3 fluorometer in 1 cm quartz cuvettes in right angle mode. Gases, reagents, and solvents were used as received unless otherwise noted. $HfCl_4$ and $Hf(cp)_2Cl_2$ were obtained from Strem Chemicals. Flash silica gel was from Sorbent Technologies. Porphyrins were obtained from Aldrich or from Frontier Scientific. All solvents and other reagents were from Aldrich. Disposable vials and test tubes were used once. All compounds had satisfactory NMR, UV−visible, and mass spectrometry data (Supporting Information).

Route 1: 1-Chloronaphthalene Solvent. Hafnium(IV) *meso*-tetraphenylporphyrinato diacetate, Hf(TPP)OAc_2. A 100 mg (0.16 mmol) amount of H_2TPP was dissolved in 4 mL of hot 1-chloronaphthalene, *ca.* 150 °C, in a 1.8 × 15.0 cm disposable test tube. The solution was allowed to cool to room temperature, and 0.32 mL of 1 M lithium hexamethyldisilizane, LiHMDA, in hexanes was added. The reaction mixture turned a dark green, indicating the formation of Li_2TPP *in situ*. The resulting amines were evaporated by heating the solution under an argon stream. A 208 mg (0.65 mmol) amount of $HfCl_4$ was added, and the mixture was allowed to reflux for 5 min. After the solution cooled, it was diluted

(19) Brand, H.; Arnold, J. *Organometallics* **1993**, *12*, 3655−3665.
(20) Brand, H.; Arnold, J. *J. Am. Chem. Soc.* **1992**, *114*, 2266−2267.
(21) Shibata, K.; Aida, T.; Inoue, S. *Tetrahedron Lett.* **1992**, *33*, 1077−1080.
(22) Kim, H. J.; Whang, D.; Kim, K.; Do, Y. *Inorg. Chem.* **1993**, *32*, 360−362.
(23) Kim, H.-J.; Whang, D.; Do, Y.; Kim, A. K. *Chem. Lett.* **1993**, *22*, 807−810.
(24) Buchler, J. W.; Heinz, G. *Chem. Ber.* **1996**, *129*, 201−205.
(25) Collman, J. P.; Kendall, J. L.; Chen, J. L.; Eberspacher, T. A.; Moylan, C. R. *Inorg. Chem.* **1997**, *36*, 5603−5608.
(26) Fryzuk, M. D.; B. Love, J.; Rettig, S. J. *Organometallics* **1998**, *17*, 846−853.
(27) Kim, H. J.; Jung, S.; Jeon, Y. M.; Whang, D.; Kim, K. *Chem. Commun.* **1999**, 1033−1034.
(28) Stulz, E.; Burgi, H. B.; Leumann, C. *Chem.-Eur. J.* **2000**, *6*, 523−536.
(29) Witowska-Jarosz, J.; Gorski, L.; Malinowska, E.; Jarosz, M. *J. Mass Spectrom.* **2002**, *37*, 1236−1241.
(30) Pistorio, B. J.; Nocera, D. G. *J. Photochem. Photobiol., A* **2004**, *162*, 563−567.
(31) Drain, C. M.; Lehn, J.-M. *Chem. Commun.* **1994**, 2313−2315 (correction 1995, p503).
(32) Drain, C. M.; Nifiatis, F.; Vasenko, A.; Batteas, J. D. *Angew. Chem., Int. Ed.* **1998**, *37*, 2344−2347.
(33) Drain, C. M. *Proc. Natl. Acad. Sci., U.S.A.* **2002**, *99*, 5178−5182.
(34) Drain, C. M.; Batteas, J. D.; Flynn, G. W.; Milic, T.; Chi, N.; Yablon, D. G.; Sommers, H. *Proc. Natl. Acad. Sci., U.S.A.* **2002**, *99*, 6498−6502.
(35) Drain, C. M.; Chen, X. Self-Assembled Porphyrinic Nanoarchitectures. In *Encyclopedia of Nanoscience & Nanotechnology*; Nalwa, H. S., Ed.; American Scientific Press: New York, 2004; Vol. 9, pp 593−616.
(36) Cheng, K. F.; Thai, N. A.; Teague, L. C.; Grohmann, K.; Drain, C. M. *Chem. Commun.* **2005**, 4678−4680.
(37) Drain, C. M.; Bazzan, G.; Milic, T.; Vinodu, M.; Goeltz, J. C. *Isr. J. Chem.* **2005**, *45*, 255−269.
(38) Drain, C. M.; Goldberg, I.; Sylvain, I.; Falber, A. *Top. Curr. Chem.* **2005**, *245*, 55−88.
(39) Diskin-Posner, Y.; Dahal, S.; Goldberg, I. *Angew. Chem., Int. Ed.* **2000**, *39*, 1288−1292.
(40) Goldberg, I. *Chem.-Eur. J.* **2000**, *6*, 3863−3870.
(41) Diskin-Posner; Patra, G. K.; Goldberg, I. *Eur. J. Inorg. Chem.* **2001**, *2001*, 2515−2523.
(42) Goldberg, I. *Cryst. Eng. Commun.* **2002**, *4*, 109−116.
(43) Diskin-Posner, Y.; Patra, G. K.; Goldberg, I. *Cryst. Eng. Commun.* **2002**, *4*, 296−301.
(44) Shmilovits, M.; Diskin-Posner, Y.; Vinodu, M.; Goldberg, I. *Cryst. Growth Des.* **2003**, *3*, 855−863.
(45) Goldberg, I. *Chem. Commun.* **2005**, 1243−1254.
(46) Lee, S. J.; Hupp, J. T. *Coord. Chem. Rev.* **2006**, *250*, 1710−1723.
(47) Chou, J.-H.; Kosal, M. E.; Nalwa, H. S.; Rakow, N. A.; Suslick, K. S. Applications of Porphyrins and Metalloporphyrins to Materials Chemistry. In *The Porphyrin Handbook*; Kadish, K.; Smith, K.; Guilard, R., Eds.; Academic Press: New York, 2000; Vol. 6, pp 43−131.
(48) Fan, J.; Whiteford, J. A.; Olenyuk, B.; Levin, M. D.; Stang, P. J.; Fleischer, E. B. *J. Am. Chem. Soc.* **1999**, *121*, 2741−2752.

in 50 mL of CH_2Cl_2, loaded directly onto 30 g of silica gel in a glass frit filter, 4.25 cm × 4.25 cm, 60 cm^3, placed on a filtering flask, and vacuum filtered. The first fraction, along with reaction solvent, was eluted with neat CH_2Cl_2 and was identified as unreacted porphyrin by UV−vis. The second fraction, Hf(TPP)-OAc_2, was eluted with CH_2Cl_2:MeOH:CH_3COOH, 3:1:1, and reduced to 1 mL of mostly acetic acid by rotary-evaporation. The product was precipitated by the addition of 10 mL of distilled water and then centrifuged. The bright pink solid was dried and weighed to yield 122 mg (82%) of the Hf(TPP)OAc_2 complex. Hf(TPP)-OAc_2: ^{1}H NMR (500 MHz $CDCl_3$) δ ppm: 9.04 (s, 8H, pyrrole), 8.38 (br, 4H, phen-*o*), 8.13 (br, 4H phen-*o*), 7.83 (m, 4H, phen-*p*), 7.79 (br m, 8H phen-*m*), 0.39 (br s, 6H OAc). UV−vis CH_2Cl_2 λ_{max} nm(log ϵ): 393(4.61), 414(5.70), 498(3.52), 540(4.39), 572-(3.44). Positive ESI-MS *m*/*z* Hf(TPP)$OAc_2(H_3O)^{+1}$ calcd 928.3, found 928.2; MALDI-MS as the dithranol ($C_{14}H_{10}O_3$) adduct: *m*/*z* Hf(TPP)$(C_{14}H_9O_3)^{+1}$ calcd 1017.5, found 1017.1.

Hafnium(IV) *meso*-tetra-4-tolylporphyrinato diacetate, Hf(TTP)-OAc_2, was synthesized by reacting of 100 mg of H_2TTP with 190 mg of $HfCl_4$ according to method 1 except that the unreacted H_2-TTP was eluted with neat toluene. The yield averaged 80%. Hf-(TTP)OAc_2: ^{1}H NMR (500 MHz $CDCl_3$) δ ppm: 9.05 (s, 8H, pyrrole), 8.25 (br, 4H phen-*o*), 8.02 (br, 4H, phen-*o*), 7.59 (br, 8H, phen-*m*), 2.75 (s, 12H, $PhCH_3$), 0.22 (s, 6H, OAc). UV−vis in CH_2-Cl_2 λ_{max} nm(log ϵ): 395(4.63), 416(5.71), 500(3.60), 539(4.43), 574(3.47). MALDI-MS as the dithranol ($C_{14}H_{10}O_3$ FW. 226) matrix adduct: found Hf(TTP)$(C_{14}H_9O_3)^{+1}$ 1074, calcd 1073.

1-Chloronaphthalene/Cresol Solvent. Hafnium(IV) *meso*-Tetra-4-pyridylporphyrinato Diacetate, Hf(TPyP)OAc_2. A 100 mg amount of H_2TPyP was dissolved in a 1.8 × 15.0 cm test tube in 5 mL of a 3:1 mixture of dry 1-chloronaphthalene and freshly distilled *o*-cresol. In a separate 1.2 × 7.5 cm test tube, 70 mg of NaH (60% dispersion in mineral oil) was added to 2 mL of *o*-cresol and heated near reflux until no further H_2 gas evolution was observed to form a *ca.* 8.5% solution of the sodium cresolate salt, which was decanted into the porphyrin solution. A rubber septum was placed on the test tube, and argon was vented via syringe needles until the vessel was fully purged. The solution was heated close to reflux. A 260 mg amount of $HfCl_4$ (5 equiv) was added, and the mixture was allowed to reflux for 20 min under a strong flow of argon. The reaction turned a deep red color, and the UV−vis indicated only small amounts of unreacted porphyrin. The reaction mixture was loaded directly onto 35 g of silica in a 4.5 cm × 4.5 cm glass frit filter on a filter flask. Washing with CH_2Cl_2 removes most of the reaction solvent, and an eluent of 10:1 v/v CH_2Cl_2:MeOH removed unreacted porphyrin. Neat methanol, followed by MeOH:H_2O 1:1 v/v, removed trace amounts of cresol while the metalated product remained unmoved at the top of the silica gel. Washing with 1:1 distilled H_2O:CH_3COOH cleanly removes the Hf(TPyP)OAc_2, wherein the pyridyl groups are protonated. A 100 mg amount of sodium acetate was added to this fraction to deprotonate the pyridinium ions, and the solvent was removed by evaporation under reduced pressure. The residue was washed three timed by suspension in 4 mL of distilled H_2O and centrifugation, and the supernatant containing excess salts was decanted. The pink solid was dried and weighed to yield 130 mg (73%) of the Hf(TPyP)OAc_2 complex. Hf(TPyP)OAc_2: ^{1}H NMR (500 MHz $CDCl_3$) δ ppm: 9.15(s, 8H, pyrrole), 9.05 (br, 8H, py-3,5 H), 8.44 (br, 4H py-2 or 6), 8.23 (br, 4H py-2 or 6), 0.92 (br s, 6H OAc). UV−vis MeOH λ_{max} nm(log ϵ): 3.96(4.60), 416(5.69), 500(2.84), 538(3.37), 570(3.49). Positive ESI-MS *m*/*z* Hf(TPyP)(HOAc)$(OMe)_2^{+1}$ calcd 918.2, found 918.2; MALDI-MS as the dithranol ($C_{14}H_{10}O_3$ FW. 226) matrix adduct: *m*/*z* Hf(TPyP)H$(C_{14}H_9O_3)_2^{+1}$ calcd 1246.6, found 1246.2.

Hafnium(IV) *meso*-tetra(4-methylbenzoate)porphyrinato diacetate, Hf(TMeCPP)OAc_2, was synthesized similarly. To 200 mg of H_2TMeCPP (0.24 mmol) in 8 mL of 1:1 1-chloronaphthalene:*o*-cresol was added 3 mL of the cresolate solution, followed by 380 mg (1.2 mmol) of $HfCl_4$. The reaction was refluxed under a flow of argon for 30 min, allowed to cool to room temperature, and precipitated with 300 mL of hexanes. The mixture was filtered, collecting most of the product as a solid, and the supernatant was added directly to a silica gel column, 35 g, 4.25 cm × 4.25 cm, in a glass frit filter connected to a vacuum filtration flask to leave a bright pink band at the top of the column. Neat CH_2Cl_2 was passed over the column, eluting a dark purple band of unreacted porphyrin and trace amounts of reaction solvent. Further elution of increasing proportions of MeOH up to 100% eluted more unreacted porphyrin with some of the ester groups saponified to the acids as indicated by TLC. A 100 mL amount of 1:1 MeOH:H_2O, followed by neat methanol, removed trace amounts of cresol from the column. The metalloporphyrin was eluted cleanly with CH_2Cl_2:MeOH:CH_3COOH, 3:1:1, and the solution reduced to 1 mL by rotary evaporation and precipitated with 20 mL of distilled water. The mixture was centrifuged, and the clear supernatant was decanted. ^{1}H NMR of the dry solid indicated that some of the methyl esters had been cleaved, so this fraction was combined with the initial precipitate (*ca.* 85% yield). Estimates from the MALDI spectrum of this mixture indicated the following proportions of benzoate groups: tri/tetra 7%; 5,10-/5,15- di 12%; mono 24%; the target tetramethyl ester 57%. The benzoate groups were reesterified to the methyl esters by reaction of the products with diazomethane prepared and distilled in diethyl ether according to standard procedures to yield 194 mg, 72% of the Hf(TMeCPP)OAc_2 complex. ESI-MS and ^{1}H NMR still indicated a small portion of carboxylates remained after the diazomethane reaction. Since the Hf(TMeCPP)OAc_2 complex is intended to aid in characterization and as a precursor to the Hf-(TCPP) complex, this was deemed satisfactory. Hf(TMeCPP)OAc_2: see Supporting Information for ^{1}H NMR. UV−vis CH_2Cl_2 λ_{max} nm-(log ϵ): 394(4.06), 416(5.12), 500(3.11), 540(3.89), 572(3.04). MALDI-MS as the dithranol matrix adduct ($C_{14}H_{10}O_3$ FW. 226): *m*/*z* Hf(TMeCPP)$(C_{14}H_9O_3)^{+1}$ calcd 1249, found 1250.

Hafnium(IV) *meso*-Tetra(4-carboxyphenyl)porphyrinato Diacetate $[Hf(TCPP)]_x$. A 25 mg amount of the Hf(T−MeCPP)OAc_2 was dissolved in 2 mL of *N*-methylpyrrolidone, NMP, and 1 g of pyridinium hydrochloride in a 10 mL screw cap vial. A 0.1 mL amount of distilled water was added, and the vial was purged with nitrogen gas. The cap was loosely sealed, and the solution was refluxed for 3 h to cleave the esters. The vial was allowed to cool to room temperature, diluted with 8 mL of water to precipitate the porphyrin complex, and centrifuged. The supernatant contained a trace amount of free base porphyrin. Two additional washes and centrifugations from water and one from acetone effectively removed the unreacted porphyrin and reaction solvents. The resulting complex was dried and weighed: 20 mg of Hf(TCPP), 93% yield. This product is a coordination polymer wherein the carboxylates on one porphyrin serve as oxo ligands on a neighboring Hf and is difficult to dissolve. The complex dissolves sparingly in DMF and moderately in MeOH, 10% NH_4OH. UV−vis in MeOH, 10% NH_4OH (which likely depolymerizes the coordination polymer to some extent) λ_{max} nm (relative intensities): 418(1), 538(0.093). MALDI mass spectrum as the dithranol matrix ($C_{14}H_{10}O_3$ FW. 226) adduct: calcd 1192.48, found Hf(TCPP)$(C_{14}H_9O_3)^{+1}$ 1192.25.

Route 2: Hf(cp)$_2$Cl$_2$ Melt. Hafnium(IV) *meso*-tetra-perfluorophenylporphyrinato diacetate, Hf(TPPF_{20})OAc_2, was synthesized by a solventless method. To a dry, screw-cap, 2 mL glass vial with 97 mg of H_2TPPF_{20} (0.1 mmol) was added 114 mg of Hf$(cp)_2Cl_2$

(0.3 mmol) that was crushed to a fine powder. The contents were mixed thoroughly by gently turning the vial. After the vial was capped, it was heated in a hot sand bath (*ca.* 300 °C) just on the bottom surface so that the sand level was never above that of the vial's contents. The $Hf(cp)_2Cl_2$ melted and solvated the porphyrin, forming a dark, molten paste. White salts and cyclopentadiene sublimed from the paste and deposited on the upper walls of the vial over the course of *ca.* 30 s. The vial was allowed to cool for *ca.* 30 s before removing the cap. The vial was then fully embedded in the hot sand for *ca.* 10 s while argon was blown gently into the vial to remove the remaining cyclopentadiene before allowing the vial to cool to room temperature.

Care was taken not to overheat the sample to minimize the formation of a reduced Hf(IV) chlorin. The residue from the vial was sonicated in 60 mL of CH_2Cl_2 in a 200 mL conical flask. A 0.1 mL amount of concd HCl was added to the solution which turned green, indicating the formation of $H_4TPPF_{20}^{2+}$ from unreacted porphyrin. The solution was added to a silica column in a glass frit filter, 4.5 cm × 4.5 cm, and eluted by vacuum filtration. Neat CH_2Cl_2 followed by a solution of CH_2Cl_2, 2% v/v triethylamine, eluted the unreacted porphyrin, followed by 1:1 $CHCl_2$:MeOH v/v to remove the last of the unreacted material. $CHCl_3$:MeOH:CH_3COOH, 77:20:3, eluted the metalated porphyrin as $Hf(TPPF_{20})OAc_2$. The product was dried and weighed: 18 mg of $Hf(TPPF_{20})OAc_2$, *ca.* 12% yield. $Hf(TPPF_{20})OAc_2$ ^1H NMR (500 MHz $CDCl_3$) δppm: 9.13 (s, 8H, pyrrole), 0.24 (s, 6H OAc). UV−vis in CH_2Cl_2 λ_{max} nm(relative intensities): 387(0.13), 408(1.0), 535(0.051), 572(0.039). MALDI-MS *m/z* $Hf(TPPF20)OAc^{+1}$, calcd 1210, found 1210.

Auxiliary Ligand Exchange. The $Hf(TTP)oct_2$ was prepared by running the corresponding acetate derivative over a small column using 70:25:5 CH_2Cl_2:EtOH:octanoic acid as eluent. The Hf(TPP)-$PABA_2$ (*p*-aminobenzoic acid) complexes were prepared from the acetate derivative by refluxing in a basic solution with PABA. Synthetic details and characterization are reported in the Supporting Information.

$[Hf(TPP)]_2(\mu\text{-}\eta^2\text{-}O_2)_2$. A 7 mg amount of $Hf(TPP)OAc_2$ was dissolved in 3 mL of $CHCl_3$ with 20% MeOH. One drop of concd aq HCl was added (to disassociate the acetate ligands and from the dichloride), and 1 mL of methanol was layered over the solution. A 0.05 mL amount of pyridine was added to the top of the methanol layer. The layers were allowed to slowly diffuse and evaporate. After two weeks, X-ray diffraction quality, square crystals of the $[Hf(TPP)]_2(\mu\text{-}\eta^2\text{-}O_2)_2$ complex formed on the walls of the glass. The crystals constituted the majority of the material. The Hf(TPP)-Cl_2 complex is hydrolyzed during the ESI-MS experiment which uses acetonitrile/methanol with <1% formic acid, to form multiple oxo-bridged species, some of which are consistent with the peroxo-bridged dimer. ESI-MS: found $[Hf(TPP)]_2[\mu\text{-}(O)(OH)]^{+1}$ *m/z* 1615, $[Hf(TPP)]_2(\mu\text{-}\eta^2\text{-}O_2)(\mu\text{-}OH)^{+1}$ *m/z* 1631, $[Hf(TPP)]_2(\mu\text{-}\eta^2\text{-}O_2)$-$(OMe)]^{+1}$ *m/z* 1645. UV−vis of a crystal in CH_2Cl_2 λ_{max} nm (relative intensities): 378(0.064), 402(1), 497(0.0067), 535(0.053), 570(0.0052).

The oxo-bridged dimer structure was formed with the Hf(TTP) complex as well. These crystals were obtained from a chloroform solution with 4% v/v concd aq HCl. ESI-MS of the $Hf(TTP)OAc_2$ also resulted in the oxo-bridged $[Hf(TTP)]_2[(\mu\text{-}O)H_3O^+$ calcd 1729, found 1729.2.

$[Hf(TTP)]_2[SO_4]_2$ and $Hf(TPP)[HPO_4]_3^{-2}$. A 2% v/v solution of concentrated sulfuric or phosphoric acid in 4:1 CH_2Cl_2:MeOH was passed over the column, and the $[Hf(TTP)]_2[SO_4]_2$ and $Hf(TPP)[HPO_4]_3^{-2}$ complexes, respectively, were eluted as one fraction. The solutions are evaporated and suspended in water followed by centrifugation to remove remaining acid. Thus, the exchange the oxo ligands is accomplished in one step.

$[Hf(TPP)]_2[SO_4]_2$. Elemental analysis found 2.7% for sulfur, 3.4% calculated for the pure compound, which confirms the presence of this element in the X-ray diffraction structure determination, but UV−visible spectra indicate that this sample also contained the hydrated complex, resulting from the exchange equilibrium with water during purification. ^1H NMR (500 MHz, dimethyl sulfoxide-d_6) δ ppm: 8.97 (s, 8 H, pyrrole), 8.40 (br, 4 H, phen-*o*), 8.14 (br, 4 H, phen-*o*), 7.88 (br m, 12 H, phen-*m*,*p*), UV−vis in $CHCl_3$ λ_{max} nm(relative intensities): 388(0.078), 411(1), 493(0.0064), 536(0.045), 568(0.0060)

$[Hf(TPP)]_2[HPO_4]_3^{-2}$. ^1H NMR (500 MHz, chloroform-*d*) δ ppm: 8.74 (s, 8 H, pyrrole), 8.12 (br m, 4 H), 7.76 (br m, 12 H), 7.62 (br m, 4 H). UV−vis in CH_2Cl_2 λ_{max} nm(relative intensities): 378(0.073), 410(1), 498(0.0072), 538(0.055), 575(0.0064). We observed a sharp singlet at −9.96 ppm in the ^{31}P NMR (400 MHz, chloroform-*d*) with an external aqueous H_3PO_4 standard at 0.0 ppm. The same sample was measured with an internal excess of H_3PO_4, showing a very broad peak centered at −10.06 ppm, due to the exchange of phosphates around the hafnium ion, and a free phosphate peak at 0.25 ppm.

Crystal Growth Conditions for Compounds 1−10. 1. Hf-(TPyP)OAc_2. Crystals of the $Hf(TPyP)OAc_2$ complex were obtained by slow evaporation (2 weeks) of the complex in a 1:1 solution of MeOH:$CHCl_3$, 2% v/v nitrobenzene.

2. Hf(TPP)$PABA_2$. Crystals of the $Hf(TPP)PABA_2$ complex came from slow evaporation of the complex in a 1:1 solution of MeOH:$CHCl_3$, 2% v/v nitrobenzene.

3. Hf(TTP)$pent_2$. The crystal structure of the pentanoate derivative, $Hf(TTP)pent_2$, was found as a result of a sample of Hf-$(TTP)Cl_2$ treated with trace amounts of pentanoic acid (<1%) during crystallization in a mixed solvent of THF and $CHCl_3$.

4. $[Hf(TPP)]_2(\mu\text{-}\eta^2\text{-}O_2)_2$. See above.

5 and 6. $[Hf(TTP)]_2(\mu\text{-}\eta^2\text{-}O_2)_2$ (Chloroform Solvate) and $Hf(TTP)]_2(\mu\text{-}\eta^2\text{-}O_2)_2$ (Nitrobenzene Solvate). The Hf(TTP) peroxo-bridged dimers formed from preliminary experiments in eluting the Hf(TTP) using dilute HCl. The samples, after elution over silica, were allowed to evaporate: one with 2% v/v nitrobenzene and one without this cosolvent, affording single crystals of the corresponding compounds.

7 and 8. $[Hf(TPP)]_2[SO_4(H_2O)]_2$ and $[Hf(TTP)]_2[SO_4(CH_3$-$OH)]_2$. Crystals of both the solvated sulfate derivatives were obtained by slow evaporation of the complexes in a 1:1 solution of MeOH:$CHCl_3$.

9. $[Hf(TTP)]_2[SO_4]_2$. Crystals of the Hf(TPP) sulfate lacking any coordinating solvents display a structure where more of the oxygens from the bridging sulfates participate in coordination to the hafnium ions to fulfill the large coordination sphere. The sample was dried for 3 days in a *ca.* 110 C oven before being dissolved in *ca.* 0.75 mL of $CDCl_3$ for NMR spectroscopy, after which 0.1 mL of nitrobenzene and 0.1 mL of acetonitrile were added to the NMR tube and the solvents slowly evaporated to form diffraction quality crystals.

10. $[Hf(TPP)]_2[HPO_4]_3^{-2}$. The phosphate derivative was crystallized from a $CHCl_3$:MeOH, 2% v/v nitrobenzene. The dimer complex has a formal negative charge most likely compensated by hydronium ions.

Results and Discussion

Synthesis and Characterization of Hafnium(IV) Porphyrinate Derivatives. Though heating the metal salts with

the free base in a high boiling solvent is common to most porphyrin metalation reactions, no single synthetic strategy is amenable to form the hafnium complexes of aryl porphyrins bearing a diverse array of functional groups because the solubility and reactivity of each macrocycle differs. Also, the yield of some methods significantly diminishes when used on <100 mg scales. These modifications in the synthetic procedures afford a variety of Hf(Por) complexes heretofore not reported. As with most metalation reactions,[17b] these routes can be divided into two strategies: (1) choosing solvent systems that result in greater solubility of the porphyrin and the metalloporphyrin products, and (2) activation of the porphyrin toward metalation by making the dianion.

An attractive feature of the routes reported herein is that the desired secondary ligands, L, of any of the $Hf(Por)L_2$ complexes are added as part of the purification procedures. This obviates the need to isolate the labile $Hf(Por)Cl_2$ formed in the metalation reaction.[19,20] The $Hf(Por)Cl_2$ complex binds tightly to silica and cannot be eluted even with neat methanol. As hafnium is quite oxophilic, we assume this is due to the exchange of chloride ligands for the available oxygens on the surface of the silica and is observed as a bright red band at the top of the silica column. This strategy facilitates removal of unreacted starting materials and reaction solvents. CH_2Cl_2, MeOH, and a small percentage of acetic acid rapidly and cleanly elutes the product as the $Hf(Por)OAc_2$ complex. An air stable, bright pink powder is obtained after removal of the solvent and precipitation with distilled water. The acetates do not exchange for water and are a favorable entry to a diverse array of derivatives with various ligands.[4,91]

Alternatively, replacing the acetic acid in the eluent in the last step of purification with other carboxylic acids directly results in the $Hf(Por)L_2$ with the corresponding carboxylate ligands in nearly quantitative yields. Unexpectedly, the addition of small amounts of sulfuric acid or phosphoric acid to the eluent results in dimers, bridged by these multitopic anions. Both the carboxylate derivatives and the sulfate and the phosphate-bridged dimers also can be formed from the $Hf(Por)OAc_2$.

The reaction vessels were disposable test tubes fitted with rubber septa or screw cap vials, obviating the need for Schlenk-ware or nitrogen boxes. The spectroscopic characterization and high-resolution mass spectrometry of all the reported complexes is consistent with the given structure and the previously reported $Hf(TPP)OAc_2$.[4,9] Also, most of the derivatives are characterized by crystallography.

Route 1. Porphyrins such as TPyP and TMeCPP are more soluble in 1-chloronaphthalene[49] or 1-chloronaphthalene/cresol compared to toluene or benzonitrile.[4] Cresol was chosen because it is high boiling and less reactive in the transesterification of esters compared to aliphatic alcohols. The macrocycles are activated toward metalation by formation of Li_2Por *in situ* with lithium hexamethyldisilazane (LiHMDS) under an inert atmosphere or Na_2Por by the cresolate in the mixed solvent system. Decomposition and side product formation are minimized by refluxing no more than 5 min for TMeCPP and 20 for TPyP. The use of both solvent systems allows direct use of $HfCl_4$ without the need to first prepare the more soluble THF or DME adducts,[22] allows greater concentrations to be used, and allows much shorter reaction times compared to reactions in benzonitrile.[4] For octaethylporphyrin, OEP, and phthalocyanines, high boiling solvents and extended reaction times lead to a significant fraction of the bis-porphyrin hafnium(IV) sandwich complex,[50] but orthogonal aryl substituents strongly inhibit sandwich complex formation using the $HfCl_4$ starting complex. After extended reflux (24 h), the sandwich complex was not observed using the methods reported here. Only a $Hf(NEt_2)_4$ reagent is reported to yield (*ca.* 50%) the Hf(IV)-TPP_2 complex.[51]

For (TMeCPP), some of the four ester groups are still cleaved to form the acids as indicated by a complex NMR spectrum and by mass spectrometry, but the crude product can be reesterified with diazomethane, which facilitates spectroscopic characterization of this product. Since the $Hf(TMeCPP)L_2$ complex serves only as a precursor to the $Hf(TCPP)L_2$ complex, which can be used to design hierarchical materials, this product was used without further purification. The potential to construct robust materials is indicated by the fact that $Hf(TCPP)L_2$ forms a coordination polymer wherein the carboxyates of one complex coordinate the Hf on other complexes.

Route 2 was developed as a rapid, solventless method to synthesize hafnium porphyrinates by melting 3 equiv of the $Hf(cp)_2Cl_2$ starting complex with the free base porphyrin. Up to 200 mg of H_2TPP can be metalated with hafnium, using only a 2 mL screw cap vial in under 2 min and provides the highest yield reported for $Hf(TPP)L_2$ (95%). For $Hf(TPPF_{20})L_2$ the yields are more modest, but in our hands no other method works without substitution of the reactive *p*-fluoro group or decomposition of the macrocycle.

For both the Hf(TPP) and $Hf(TPPF_{20})$ complexes, careful control of the reaction temperature is needed to (1) minimize the formation of a small fraction of a reduced Hf(Por) complex, which was identified as the metallochlorin characterized by a low-energy visible absorbance around 630 nm with significantly greater intensity than the normal porphyrin Q bands, and (2) minimize polymerization of the excess cyclopentadienyl hafnium salts.

Derivatives. The facile exchange of the counterion ligands can bring functionality to the $Hf(Por)^{2+}$ parent complexes. Scheme 1 shows the general methods for the derivatives in the crystal structures below. We focus on the more stable[9] bidentate carboxylate ligands and polyatomic oxo-anions to satisfy both the charge and the hafnium coordination sphere. When labile, monodentate anionic ligands are used, coordinating solvents fill the empty coordination sites and different spectroscopic signatures are observed that depend

(49) Collman, J. P.; Kendall, J. L.; Chen, J. L.; Collins, K. A.; Marchon, J. C. *Inorg. Chem.* **2000**, *39*, 1661−1667.

(50) Guilard, R.; Barbe, J.-M.; Ibnlfassi, A.; Zrineh, A.; Adamian, V. A.; Kadish, K. M. *Inorg. Chem.* **1995**, *34*, 1472−1481.

(51) Girolami, G. S.; Milam, S. N.; Suslick, K. S. *Inorg. Chem.* **1987**, *26*, 343−344.

Scheme 1 [a]

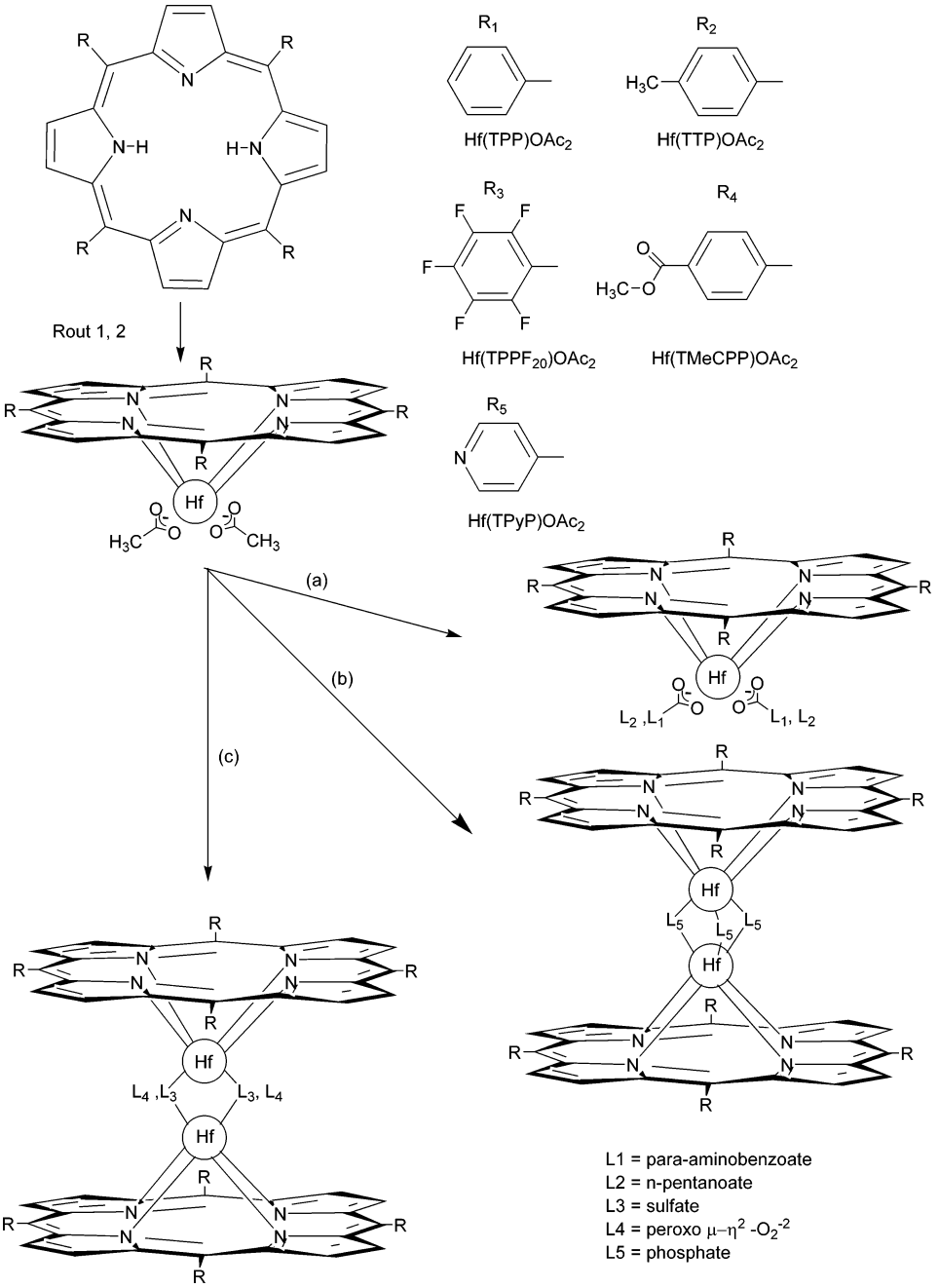

[a] R = R_1, R_2, R_3, R_4, R_5 and L = L_1, L_2, L_3, L_4, L_5. Route 1: for R_1, R_2, R_3, R_5 (i) porphyrin in 1-chloronaphthalene; (ii) LiHMDS; (iii) $HfCl_4$, reflux 5 min; (iv) adsorb onto silica gel and elute with 3−5% HOAc. For R_1, R_2, R_5 (i) porphyrin in 1-chloronaphthalene, *o*-cresol; (ii) 10 equiv of sodium cresolate; (iii) $HfCl_4$; (iv) adsorb onto silica gel and elute with HOAc. Route 2: for R_1, R_2, R_3 (i) porphyrin + $Hf(cp)_2Cl_2$; (ii) Melt at *ca.* 300 °C; (iii) dissolve in CH_2Cl_2; (iv) adsorb onto silica gel and elute with 3−5% HOAc. Starting with $Hf(Por)OAc_2$ a variety of derivatives can be made by ligand exchange (a) with an excess of another carboxylate, (b) with an excess of phosphate, and (c) with an excess of sulfate or an aqueous acid in air.

on solvent and water content. During precipitation and centrifugation from water, these derivatives are stable to ligand hydrolysis.

The sulfate-, phosphate-, and peroxo-bridged dimers are a unique set of compounds. The reported zirconium(IV) porphyrinate oxo-bridged crystals are formed by hydrolysis of the $Zr(Por)Cl_2$ or $Zr(Por)R_2$ where R = CH_3[2] or $(CH_2)_3$-CH_3,[1,9] by simple exposure to atmosphere. Aqueous precipitation on the $Hf(Por)Cl_2$ complex causes immediate hydrolysis of a large portion of the sample as indicated by a large absorbance peak near 401 nm in the UV−vis spectrum consistent with literature values for the oxo-bridged species formed in the presence of pyridine.[19] Treating $Hf(TPP)OAc_2$ with a small quantity of dilute HCl to dissociate the acetate ligands followed by a layer of pyridine to slowly neutralized the acid affords the peroxo-bridged dimeric complex, $[Hf(TPP)]_2(\mu\text{-}\eta^2\text{-}O_2)_2$, as a crystalline product after the solvent is allowed to evaporate. Spectroscopic and crystallographic evidence, *vide infra*, indicates this procedure results in a peroxo-bridged ($\mu\text{-}\eta^2\text{-}O_2^{-2}$) dimer in contrast to the previously reported hydroxyl/oxo-bridged dimer.[3,6,54] Metalloporphyrins with first-row redox active metals (e.g., Fe(II)TPP

and Mn(II)TPP) are known to bind dioxygen to form single η^1 peroxo-bridged dimers which then further react in the presence of oxygen and water to form the μ oxo dimers.[17c] The exact redox chemistry leading to our peroxo-bridged complex is not known at this time and is the subject of continuing investigations.

The sulfate-bridged complex, $[Hf(TPP)]_2(SO_4)_2$, and the phosphate derivative, $[Hf(TPP)]_2(HPO_4)_3$ dianion (water bridges to the phosphate and/or H_3O^+counterions), are the first of their kind to be reported for either hafnium or zirconium porphyrinates. The sulfate-bridged dimer was also found for the Hf(TTP) complex (see Crystallographic Discussion). The dimeric structures are observed by crystallography using crystals from multiple, independent preparations. NMR and mass spectrometry indicate the purity of the compounds. Considering the large excess of phosphate or sulfate ions (2% v/v of H_2SO_4 or H_3PO_4) during the preparation and crystallizations, and that only the dimeric structures are found rather than the monomers, the sulfate- and phosphate-bridged dimers must be thermodynamically favored products. These bridged complexes are also somewhat resistant to hydrolysis, since precipitation from water to remove excess salts results in a poorly defined high energy shoulder of the Soret band in the UV−visible spectra. A structure obtained from crystals from a partially hydrolyzed sample of the sulfate derivative shows the water solvate.

Spectroscopy. Mass Spectroscopy. For the diacetate complexes, we observed a number of mass peaks in the ESI-MS relating to the exchange of acetate for methanol and water ligands in the eluent (1% formic acid in methanol). The major peaks observed in the ESI-MS of $Hf(TPP)Cl_2$ indicate that the oxo-bridged species formed in the ESI-MS. We interpret the observed *m*/*z* peak at 1631 as consistent with a peroxo-bridged $Hf(TPP)]_2(\mu\text{-}\eta^2\text{-}O_2)(OH^-)]^+$, which is derived from the bis $(\mu\text{-}\eta^2\text{-}O_2)$-bridged species, rather than a combination of H_2O, OH^-, or μ-oxo (O^{-2}) species. For example, the *m*/*z* of $[Hf(TPP)]_2[(OH)_3]^{+1}$ is calculated to be 1633. Previous examples of oxo-bridged porphyrinate complexes also indicate an oxide bridging unit observed by mass spectroscopy, e.g., the $Sc(OEP)]_2[\mu\text{-}O]^{+1}$ species[36] where the bridging oxygen was formally assigned as an O^{2-} anion. Though ligand exchange and redox processes can occur in the ESI-MS, these results are consistent with the electronic spectra of the $[Hf(TPP)]_2(\mu\text{-}\eta^2\text{-}O_2)_2$ complex and indicate this structure persists in solution and in the solid-state crystal.

Electronic Spectroscopy. The UV−visible spectra for the hafnium porphyrinate dicarboxylate complexes are generally characterized by a large Soret band between 414 and 416 nm and a *ca.* 15-fold less intense Q-band near 540 nm, flanked on either side by smaller Q-bands of even lesser intensity.[4] The optical spectra of the sulfate- and phosphate-bridged dimer complexes generally have Soret bands near 408 nm and Q-bands that are both 3−5 nm to the blue of the corresponding monomeric carboxylic derivatives. These spectral features are consistent with the blue shifts found for face-to-face dimers[55] and $M(Por)_2$ sandwich complexes.[7,56] The inorganic anions, SO_4^{-2} and HPO_4^{-2}, may cause the observed blue shifts simply by donation of electron density into the porphyrin core via the Hf without dimer formation, but the previously reported $Hf(TPP)(P_3O_9^{-3})[TBA]$ (TBA= tetrabutyl ammonium cation), which has a Soret band at 412 nm,[1] is not significantly blue-shifted compared to the dichloride starting complex.[1] The complex with the electron-rich $P_3O_9^{-3}$ ligand is incapable of bridging two porphyrin units and so is a monomer in the crystal structure and has a Soret band more typical of monomeric hafnium porphyrinates. Thus, the SO_4^{-2}, and HPO_4^{-2} mediate electronic communication between the chromophores since the distance between the two macrocycles is too great for strong $\pi-\pi$ interactions.

The $[Hf(TPP)]_2(\mu\text{-}\eta^2\text{-}O_2)_2$ complex has a significantly blue-shifted Soret band near 401 nm, while the aquo $Hf(TPP)(OH)_2$ species has a Soret near 414 nm. The observation of both bands in solution is consistent with previous accounts and the dimer/monomer equilibrium.[56] We interpret the blue-shifted peak at 401 nm as a result of dimer formation and as evidence of the peroxo, rather than hydroxy, bridging ions in solution, i.e., $[Hf(TPP)]_2(\mu\text{-}\eta^2\text{-}O_2)_2$. In previous reports, the formation of oxo-bridged dimers of Hf(Por) (oxo O^{2-}, or hydroxy OH^-) were characterized by a *ca.* 20 nm blue shift of the Soret band.[57] Thus, the greater blue shifts are indicative of greater electronic coupling arising from both the smaller bridging oxo species and face-to-face $\pi-\pi$ electronic interactions.

Fluorescence. As opposed to what is observed for open shell metalloporphyrins such as Ni(II)Por,[60,61] Hf is a closed shell group (IV) metal so ligand to metal charge transfer and excited-state metal electron configurations are unlikely. $Hf(TPP)OAc_2$ in degassed toluene is reported[5] to have a weak fluorescence with an emission maximum at 633 nm, $\Phi_f = 0.001$, with a weak shoulder to the red arising from heavy atom enhanced phosphorescence at 718 nm $\Phi_p = 8 \times 10^{-5}$. The observed fluorescence of the oxo-bridged species $[Hf(TPP)]_2(\mu\text{-}\eta^2\text{-}O_2)_2$ λ_{max} (relative intensity), 551 nm (1), 579 nm (3.1), and 633 (9.2), is significantly stronger than found for the other species. The observed fluorescence spectra for all the Hf porphyrinate complexes are remarkably similar, thus indicating that they are dominated by the presence of

(52) Bernstein, P. A.; Lever, A. B. P. *Inorg. Chem.* **1990**, *29*, 608−616.
(53) Johnson, T. J.; Disselkamp, R. S.; Su, Y.-F.; Fellows, R. J.; Alexander, M. L.; Driver, C. J. *J. Phys. Chem. A* **2003**, *107*, 6138−6190.
(54) Arnold, J.; Hoffman, C. G.; Dawson, D. Y.; Hollander, F. J. *Organometallics* **1993**, *12*, 3645−3654.
(55) Ojadi, E.; Selzer, R.; Linschitz, H. *J. Am. Chem. Soc.* **1985**, *107*, 7783−7784.
(56) Buchler, J. W.; Schneehage, Z. *Naturforsch.* **1973**, B28, 433.
(57) Ghiladi, R. A.; Ju, T. D.; Lee, D.-H.; Moenne-Loccoz, P.; Kaderli, S.; Neuhold, Y.-M.; Zuberbuhler, A. D.; Woods, A. S.; Cotter, R. J.; Karlin, K. D. *J. Am. Chem. Soc.* **1999**, *121*, 9885−9886.
(58) Seybold, P. G.; Gouterman, M. *J. Mol. Spectrosc.* **1969**, *31*, 1−13.
(59) Lee, W. A.; Grätzel, M.; Kalyanasundaram, K. *Chem. Phys. Lett.* **1984**, *107*, 308−313.
(60) Drain, C. M.; Gentemann, S.; Roberts, J. A.; Nelson, N. Y.; Medforth, C. J.; Jia, S.; Simpson, M. C.; Smith, K. M.; Fajer, J.; Shelnutt, J. A.; Holten, D. *J. Am. Chem. Soc.* **1998**, *120*, 3781−3791.
(61) Retsek, J. L.; Drain, C. M.; Kirmaier, C.; Nurco, D. J.; Medforth, C. J.; Smith, K. M.; Sazanovich, I. V.; Chirvony, V. S.; Fajer, J.; Holten., D. *J. Am. Chem. Soc.* **2003**, *125*, 9787−9800.

Table 1. Crystallographic Data for Compounds **1**−**3**

	Hf(TPyP)OAc_2	Hf(TPP)$PABA_2$	Hf(TTP)$pent_2$[a]
compound no.	**1**	**2**	**3**
empirical formula	$C_{44}H_{30}HfN_8O_4$	$C_{70}H_{52}HfN_8O_9$	$C_{58}H_{54}HfN_4O_4$
structure data file	X1590l_1	X1594l_2	X1579i_3
formula wt	913.25	1327.69	1049.54
cryst system	monoclinic	monoclinic	monoclinic
space group	*C*2/c	$P2_1$/n	$P2_1/c$
unit cell			
a/Å	14.797(3)	14.622 (3)	16.191(3)
b/Å	16.384(3)	31.050 (6)	23.452(5)
c/Å	14.984(3)	14.712 (3)	16.340(3)
α/deg	90	90	90
β/deg	93.24(3)	119.58 (3)	116.88(3)
γ/deg	90	90	90.00
V/Å^3	3626.9(13)	5809 (2)	5534.3(24)
Z	4	4	4
ρ_{calcd} [g cm^{-3}]	1.672	1.518	1.261
(Mo Kα) mm^{-1}	2.935	1.865	1.930
T/K	100	100	100
F(000)	1816	2688	2136
crystal size [mm^3]	0.56 × 0.07 × 0.07	0.40 × 0.36 × 0.18	0.40 × 0.12 × 0.10
θ range [deg]	3.23 to 27.53	2.07 to 27.48	2.96 to 27.48
index ranges	$-19 \le h \le 19$	$-12 \le h \le 18$	$-21 \le h \le 20$
	$-21 \le k \le 21$	$-38 \le k \le 40$	$-30 \le k \le 30$
	$-19 \le l \le 19$	$-18 \le l \le 10$	$-21 \le l \le 20$
reflns collected	26545	25788	59134
unique reflections	4159	11570	12600
R(int)	0.094	0.065	0.065
completeness to θ_{max} [%]	99.3	87.0	99.4
reflns with [$I > 2\sigma(I)$]	3620	8999	9144
data/restraints/parameters	4159/0/259	11570/0/793	12600/0/610
final *R* indices [$I > 2s(I)$]			
*R*1	0.034	0.040	0.049
*wR*2	0.064	0.082	0.113
R indices (all data)			
*R*1	0.046	0.061	0.074
*wR*2	0.069	0.088	0.121
largest diff peak and trough [eÅ^{-3}]	1.03 and -1.43	0.74 and -1.14	1.53 and -0.69

[a] Excluding the severely disordered THF solvent, which could not be modeled reliably by discrete atoms. Its contribution was subtracted from the diffraction data by the Squeeze procedure with the aid of the Platon software.[43]

small quantities of the peroxo (or oxo)-bridged species in these solutions.

Crystallographic Discussion. Single crystals suitable for X-ray diffraction analysis were obtained with TPP, TPyP, and TTP scaffolds, which exhibit similar metal coordination features of their central macrocyclic core. Crystallographic data for all 10 structures are given in Tables 1−3. Hafnium-(IV) d^0 ions are often characterized by high coordination numbers[62] of 7−8 with a square-antiprismal coordination environment in the latter case. Hf(IV) complexes with tetradentate porphyrin ligands in 1:1 ratio are known.[2,4,22] The Hf(IV) resides well outside the mean plane of the porphyrin core to accommodate the high coordination number required by this metal ion, rather than the larger ionic radius in of itself. This is indicated by comparison of the ionic radius of Hf(IV) (72 pm for four-coordinate, 85 pm for six-coordinate, and 97 pm for eight-coordinate) to that of Zn(II) (78 pm for four-coordinate, 88 pm for six-coordinate)[63] which resides nearly in the mean plane of the porphyrin.[64]

The high oxophilicity of early transition metals such as Hf facilitates complexation of a variety of organic as well as inorganic O-containing anions, which are used also to balance the net (2+) charge of the Hf−porphyrin adduct. These structures exist either as monomeric complexes when the auxiliary metal ion ligands are monotopic (e.g., acetate, pentanoate) or as dimers when the auxiliary ligands are multitopic (e.g., phosphate, sulfate). Structural examples with the various Hf(Por)$(L)_n$ complexes (L = oxo-ligand, $n = 2$ or 3) are provided below.

The Hf(TPyP)$(OAc)_2$, Hf(TPP)$(PABA)_2$, and Hf(TTP)-$pent_2$ compounds (**1**, **2**, and **3**, respectively) represent the first kind of monomeric complexes. Since the overall molecular structure of **1**, **2**, and **3** is similar to that of the Hf(TPP)$(OAc)_2$ complex,[4] irrespective of the different identity of the porphyrin building blocks, they will be discussed only briefly. Complexes **1**, **2**, and **3** are characterized by a pyramid-like structure, and exhibit C_2 symmetry (Figure 1). The porphyrin core adopts a distorted saddle-type conformation, with the four inner pyrrole N-atoms deviating from the C_{20}-macrocycle toward the Hf ion, which lies above it. In all three structures the distance of the hafnium ion from the mean N_4-plane is about 1.0 Å. From the other side, the metal cation is approached by the four O-sites of the carboxylate ion O-atoms at a distance of *ca.* 1.4 Å. Thus, the coordination number (CN) of the Hf ion is 8 (Table 4). In the corresponding crystals, molecules of the given complex are arranged

(62) Cotton, F. A.; Wilkinson, G. *Advanced Inorganic Chemistry*; John Wiley & Sons: New York, 1999.
(63) www.webelements.com.
(64) Scheidt, W. R.; Mondal, J. U.; Eigenbrot, C. W.; Adler, A.; Radonovich, L. J.; Hoard, J. L. *Inorg. Chem.* **1986**, *25*, 795−799.

Table 2. Crystallographic Data for Compounds **4**−**7**

	$[Hf(TPP)]_2(\mu\text{-}\eta^2\text{-}O_2)_2$	$[Hf(TTP)]_2(\mu\text{-}\eta^2\text{-}O_2)_2$ $CHCl_3$ solv	$[Hf(TTP)]_2(\mu\text{-}\eta^2\text{-}O_2)_2$ $C_6H_5NO_2$ solv	$[Hf(TPP)]_2[SO_4(H_2O)]_2$
compound no.	**4**	**5**	**6**	**7**
empirical formula	$C_{44.25}H_{29}HfN_4O_{2.25}$	$C_{49}H_{37}Cl_3HfN_4O_2$	$C_{54}H_{41}HfN_5O_4$	$C_{47}H_{39}Cl_3HfN_4O_7S$
structure data file	X1572l_4	X1592l_5	X1595l_6	X1588l_7
formula wt	831.20	998.67	1002.41	1088.72
crystal system	monoclinic	monoclinic	monoclinic	triclinic
space group	$P2_1/n$	$P2_1/c$	$P2_1/c$	$P\bar{1}$
unit cell				
a/Å	13.460(3)	14.192 (3)	14.056 (3)	11.951(2)
b/Å	12.954(3)	19.046 (4)	19.193 (4)	14.653(3)
c/Å	20.811(4)	15.641 (3)	16.056 (3)	14.865(3)
α/deg	90	90	90	66.15(3)
β/deg	107.87(3)	94.27 (3)	94.74 (3)	86.36(3)
γ/deg	90	90	90	67.92(3)
V/Å^3	3553.5(14)	4216.1 (14)	4316.7 (15)	2194.2(12)
Z	4	4	4	2
ρ_{calcd} [g cm^{-3}]	1.599	1.573	1.542	1.648
(Mo Kα) mm^{-1}	3.067	2.710	2.472	2.665
T/K	100	100	100	100
F(000)	1646	1992	2016	1088
crystal size [mm^3]	0.2 × 0.16 × 0.12	0.18 × 0.18 × 0.02	0.20 × 0.20 × 0.09	0.40 × 0.24 × 0.10
θ range [deg]	2.06 to 27.52	1.79 to 27.48	1.80 to 27.49	1.85 to 27.64
index ranges	$-17 \le h \le 17$	$-18 \le h \le 13$	$-11 \le h \le 18$	$-15 \le h \le 15$
	$-16 \le k \le 16$	$-24 \le k \le 23$	$-24 \le k \le 23$	$-19 \le k \le 19$
	$-27 \le l \le 26$	$-19 \le l \le 20$	$-20 \le l \le 20$	$-19 \le l \le 19$
reflns collected	26668	37708	34675	23739
unique reflections	7890	9630	9879	9648
R(int)	0.048	0.128	0.048	0.082
completeness to θ_{max} [%]	99.2	99.5	99.7	94.3
reflns with [$I > 2\sigma(I)$]	7142	6049	8109	8976
data/restraints/parameters	7890/0/480	9630/0/536	9879/0/581	9648/0/572
final R indices [$I > 2\sigma(I)$]				
R1	0.050	0.059	0.038	0.044
wR2	0.100	0.088	0.087	0.106
R indices (all data)				
R1	0.057	0.123	0.052	0.048
wR2	0.102	0.105	0.094	0.108
largest diff. peak and trough [eÅ^{-3}]	1.48 and -0.97	1.10 to -0.83	0.97 and -0.91	2.66 and -2.43

next to one another in flat layers, as frequently observed earlier for other metalloporphyrin compounds, exhibiting typical antiparallel face-to-face (at about 3.5 Å) or edge-to-face dispersion interactions between the peripheral aryl substituents of adjacent species.[66] Complex **1** crystallized in a solvent-free form, while complexes with the larger ligands yielded solvated structures, with water and nitrobenzene (that weakly hydrogen bond to the amino functionality of PABA associated with neighboring complexes, Table 5) in **2** and with tetrahydrofuran in **3** (see Supporting Information for a more detailed discussion and illustration of the crystal structures).

When the oxo ligands that interact with the Hf ions also possess oxygen atoms pointing in opposite directions, formation of bridged dimeric metalloporphyrin moieties becomes feasible.[2,4,22] This is the case with the bis-peroxo-bridged porphyrin dimers, $[Hf(TPP)]_2(\mu\text{-}\eta^2\text{-}O_2)_2$ (**4**) and for two structures of the tolyl derivative $[Hf(TTP)]_2(\mu\text{-}\eta^2\text{-}O_2)_2$ (chloroform solvate **5**, and nitrobenzene solvate **6**), which represent the second class of compounds in this study (Figure 2). Previous accounts have reported oxo-bridged dimers as each oxygen existing as a OH^- and/or divalent O^{-2} for Zr(IV) and Hf(IV).[2,3,9,23] Structures of three different $[Hf(Por)]_2(\mu\text{-}\eta^2\text{-}O_2)_2$ reveal consistently that the four oxygen atoms are in a rectangular geometry with bonding O−O and nonbonding O···O distances of *ca.* 1.6 and 2.5 Å, respectively. Although in the $[Hf(TPP)]_2(\mu\text{-}\eta^2\text{-}O_2)_2$ complex there is partial disorder within these sites, the two pairs of high occupancy (0.75) oxygen atoms are within the appropriate distance for O−O peroxide bonds, *ca.* 1.56 Å. The fact that this geometry is observed in three independent crystal structures differing in both solvent and/or porphyrin unit, coupled with the mass spectrometry and absorption spectra data, indicates that the present structures are appropriately viewed as peroxo-bridged dimers rather than hydroxyl- or μ-oxo-bridged entities.

In previous accounts of a tri-oxo-bridged zirconium structure,[23] the oxygens are disordered, and the structure is presented as nearly equally spaced geometries of the bridging oxygens according to their respective occupancies. Additional structures of equal probability could also be proposed for this complex where two of the bridging oxygens are close enough to be bonded as a peroxo molecule, suggesting a $[Zr(OEP)]_2[(\mu\text{-}\eta^2\text{-}O_2)(\mu\text{-}O)]$ complex. The IR spectra display stretches of 3740 cm^{-1} for the Zr(TPP) oxo-bridged crystals,[23] which can more reasonably be interpreted as a peroxide IR stretch, as this is a fairly high wavenumber for a (OH^{-1}).[67] We have not observed a tri-oxo-bridged species for the

(65) Scheidt, W. R.; Lee, Y. A. *Struct. Bond.* **1987**, *64*, 1−70.
(66) Bym, M. P.; Curtis, C. J.; Hsiou, Y.; Khan, S. a. d. I.; Sawin, P. A.; Tendick, S. K.; Terzis, A.; Strouse, C. E. *J. Am. Chem. Soc.* **1993**, *115*, 9480−9497.
(67) Engdahl, A.; Nelander, B. *Phys. Chem. Chem. Phys.* **2000**, *2*, 3967−3970.

Table 3. Crystallographic Data for Compounds **8**−**10**

	$[Hf(TTP)]_2[SO_4(CH_3OH)]_2$	$[(TPP)Hf(SO_4)]_2$	$[Hf(TPP)]_2(HPO_4)_3^{-2}$
compound no.	**8**	**9**	**10**
empirical formula	$C_{50.50}H_{40}Cl_{4.5}HfN_4O_5S$	$C_{53}H_{33}HfN_{6.50}O_6S$	$C_{89.5}H_{57}Cl_3Hf_2N_8O_{16.5}P_3$
structure data file	X1580i_8	X1570i_9	X1600l_10
formula wt	1152.94	1067.41	2064.67
crystal system	monoclinic	triclinic	monoclinic
space group	$P2_1/c$	$P\bar{1}$	$C2/c$
unit cell			
a/Å	14.624 (3)	13.244(3)	21.067(4)
b/Å	21.489 (4)	13.505(3)	15.382(3)
c/Å	15.044 (3)	13.567(3)	55.378(11)
a/deg	90	74.91(3)	90
b/deg	91.37 (3)	67.62(3)	91.60(3)
g/deg	90	79.54(3)	90
V/Å^3	4726.3 (16)	2157.1(10)	17938(6)
Z	4	2	8
ρ_{calcd} [g cm^{-3}]	1.620	1.643	1.529
(Mo Kα) mm^{-1}	2.558	2.530	2.525
T/K	100	100	100
F(000)	2302	1065	8176
crystal size [mm^3]	0.13 × 0.10 × 0.02	0.22 × 0.18 × 0.15	0.08 × 0.08 × 0.02
θ range [deg]	2.94 to 25.00	3.06 to 27.48	2.94 to 25.00
index ranges	$-17 \le h \le 17$	$-17 \le h \le 16$	$-25 \le h \le 25$
	$-25 \le k \le 25$	$-17 \le k \le 17$	$-18 \le k \le 18$
	$-17 \le l \le 17$	$-17 \le l \le 17$	$-65 \le l \le 65$
reflns collected	67862	35670	93550
unique reflections	8292	9842	15751
R(int)	0.154	0.065	0.155
completeness to θ_{max} [%]	99.7	99.4	99.5
reflns with [$I > 2\sigma(I)$]	5817	8806	10581
data/restraints/parameters	8292/0/628	9842/0/644	15751/0/1106
final R indices [$I > 2\sigma(I)$]			
$R1$	0.069	0.034	0.087
$wR2$	0.112	0.069	0.173
R indices (all data)			
$R1$	0.111	0.042	0.140
$wR2$	0.126	0.072	0.196
largest diff. peak and trough [eÅ^{-3}]	1.23 and -0.81	1.51 and -0.95	1.59 and -1.60

hafnium analogue; this may be due to the larger coordination sphere of hafnium and/or differences in experimental conditions. We do not propose to argue with the reported analysis given by the authors but suggest another possible interpretation that was not discussed. Unfortunately the diffraction data cannot define the presence or absence of hydrogen atoms, but the mass spectra of the complexes discussed herein indicate that the bridging oxygen atoms are peroxides (or oxygen radicals) in order to justify both charge and mass. Significantly, the disulfide- and diselenide-bridged dimers of Hf(TPP) were reported to have similar rectangular geometries for the sulfur and selenium atoms and so were assigned as disulfide and diselenide bridges, respectively, rather than the monoatomic bridging ions.[10] We interpret our spectroscopic data for the peroxo-bridged dimers to be consistent with these chalogen analogues. The complex pH and photosensitive redox chemistry of metalloporphyrins in the presence of oxygen and water has been studied.[17b,c]

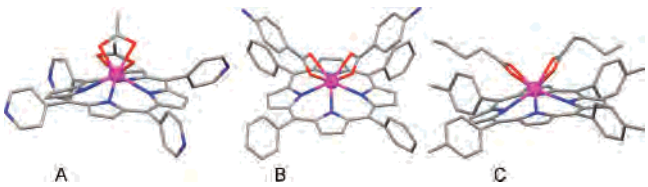

Figure 1. Molecular structures of (a) $Hf(TPyP)OAc_2$, (b) $Hf(TPP)PABA_2$, and (c) $Hf(TTP)pent_2$, showing their pyramid-like shape (H-atoms are omitted).

Because of the complexity of hafnium porphyrin redox chemistry, the peroxo-bridged compounds may arise from the reduction of O_2 from air with a sacrificial reductant (e.g., the pyridine) during the *ca.* two weeks of crystallization.[17d]

In the three bridged structures, $[Hf(Por)]_2(\mu\text{-}\eta^2\text{-}O_2)_2$, molecules of the dimeric units reside on centers of crystallographic inversion. The two peroxo bridges balance the charge of the two metalloporphyrin species. These structures are characterized by two approximate square-antiprismatic environments about each of the Hf centers, with the four bridging O-atoms forming one, common, four-sided face where the peroxo pairs form a rectangle rather than a square. The four N-atoms of the porphyrin ring comprise the other face on both sides (Table 4). As observed earlier for the Zr analogues of TPP,[23] the porphyrins are eclipsed. This group of isostructural $[Hf(Por)]_2(\mu\text{-}\eta^2\text{-}O_2)_2$ (Por = TPP or TTP) compounds is represented in Figure 2 by the molecular structure of $[Hf(TTP)]_2(\mu\text{-}\eta^2\text{-}O_2)_2$. The two peroxo ligands reside on a median plane between, and at an equal distance from, the two metalloporphyrin components. The dimer molecules in $[Hf(Por)]_2(\mu\text{-}\eta^2\text{-}O_2)_2$ form layered arrangements perpendicular to the longest axis of the corresponding unit cell (Figure 2). Adjacent layers are stacked in an offset manner, where the individual porphyrin moieties adopt slightly different orientations. The crystallization solvent (traces of methanol in $[Hf(TPP)]_2(\mu\text{-}\eta^2\text{-}O_2)_2$, chloroform, and

Table 4. Geometry of Coordination Interactions in Solids **1**−**10**[a] (Detailed information on individual contacts is given in the Supporting Information CIF files.)

Coordination Bonding Distance Range (Å)					
compounds	**1**[b]	**2**[b]	**3**[b]	**4**[b]	**5**[b]
Hf−N(pyrrole)	2.262−2.267	2.238−2.275	2.231−2.260	2.220−2.253	2.220−2.257
Hf−O(ligand)[a]	2.238−2.243	2.237−2.256	2.232−2.286	2.177−2.181	2.137−2.150
compounds	**6**[b]	**7**[c]	**8**[c]	**9**[d]	**10**[e]
Hf−N(pyrrole)	2.229−2.263	2.229−2.251	2.215−2.234	2.198−2.234	2.250−2.279
Hf−O(ligand)[a]	2.143−2.154	2.084−2.249	2.087−2.293	2.084−2.185	2.044−2.124
Deviation of Hf from the Mean Plane of the N_4(pyrrole) and O_3/O_4 (ligand) sites (Å)					
compounds	**1**[b]	**2**[b]	**3**[b]	**4**[b]	**5**[b]
N_4 (pyrrole)	1.036	1.027	1.004	0.967	0.964
O_4 (ligand)	1.437	1.430	1.452	1.564	1.559
compounds	**6**[b]	**7**[c]	**8**[c]	**9**[d]	**10**[e]
N_4 (pyrrole)	0.978	0.994	0.971	0.938	1.048, 1.054
O_3/O_4 (ligand)	1.551	1.459	1.456	1.518	1.374, 1.340
Hf−Hf Distance in the Dimeric Structures (Å)					
compounds	**1**[b]	**2**[b]	**3**[b]	**4**[b]	**5**[b]
	--	--	--	3.129	3.118
compounds	**6**[b]	**7**[c]	**8**[c]	**9**[d]	**10**[e]
	3.103	5.496	5.462	5.179	5.166

[a] The O-ligating anionic sites that balance the charge on Hf consist of two acetyl (**1**), two benzoate (**2**), two pentanoate (**3**), four hydroxy (**4**, **5**, and **6**), two SO_4^{2-} (**7**, **8**, and **9**), and three phosphate (**10**) species. [b] In **1**−**6** each of the Hf ions is characterized by coordination number of 8, coordinating to four pyrrole N-atoms of the porphyrin and four O-sites of the two carboxylate or four hydroxy ligands. [c] In **7** and **8** the Hf ion has a coordination number of 7, coordinating to four pyrrole N-atoms of the porphyrin, two O-sites (one from each sulfate ion) at *ca.* 2.08−2.15 Å, and an additional water/methanol ligand at a slightly longer distance of *ca.* 2.25−2.29 Å. [d] In **9** the Hf ion has a coordination number of 7, coordinating to four pyrrole N-atoms of the porphyrin, two O-sites of one sulfate ion, and one O-site of the second sulfate species. [e] In **10** the Hf ions have a coordination number of 7, coordinating to four pyrrole N-atoms of the porphyrin, and single O-sites of the three phosphate species. The two halves of **10** are crystallographically independent.

Table 5. Hydrogen Bonding Interactions in **2**, **7**, **8**, and **10**

D−H	A	D−H (Å)	H···A (Å)	D···A (Å)	D−H···A (Å)
		complex **2**			
NHa(64)[a]	O90 $(1-x, -y, 2-z)$[b]	0.88	2.34	3.110	171
NHb(64)[a]	O82 $(1-x, -y, 1-z)$[c]	0.88	2.48	3.349	171
NHa(74)[d]	O81 $(-x, -y, 1-z)$[c]	0.88	2.27	3.101	158
NHb(74)[d]	O90 $(-x, -y, 2-z)$[b]	0.88	2.35	3.095	143
OHa(90)[b]	O91[e]	0.85	2.19	2.977	153
OHb(90)[b]	O62[f]	0.85	2.21	2.934	143
		complex **7**			
OHa(5)[g]	O71$(-x, 1-y, 1-z)$[h]	0.84	1.81	2.619	162
OHb(5)[g]	O4[i]	0.85	1.93	2.698	149
OH(71)[h]	O81[h]	0.84	1.88	2.717	178
OH(81)[h]	O3[i]	0.84	1.95	2.781	170
		complex **8**			
OH(11)[j]	O4$(-x, 1-y, 1-z)$[i]	0.84	1.78	2.617	176
		complex **10**[l]			
OHa(41)[b]	O23[k]			2.544	
OHb(41)[b]	O34[k]			2.802	
OHa(43)[b]	O24$(x-1/2, y-1/2, z)$[k]			2.678	
OHb(43)[b]	O14$(x-1/2, y-1/2, z)$[k]			2.849	
OH91[h]	O13[k]			2.899	
OH91[h]	O33[k]			2.774	

[a] NH_2 function of first ligand. [b] Water solvent. [c] First nitrobenzene solvent. [d] NH_2 function of second ligand. [e] Second nitrobenzene solvent. [f] COO group of first ligand. [g] Water coordinated to Hf. [h] Methanol solvent. [i] Sulfate ion. [j] Methanol coordinated to Hf. [k] Phosphate ion. [l] Solution of this structure was not adequately precise to allow the location of the H-atoms.

nitrobenzene in $[Hf(TTP)]_2(\mu\text{-}\eta^2\text{-}O_2)_2$) is accommodated in the interface between adjacent porphyrin molecules.

An interesting expansion of the above concept uses the tetrahedral geometry of SO_4^{2-} anions to bridge two Hf(Por) complexes, thus providing another useful bridging element for the formation of the metalloporphyrin dimers. The successful synthesis of the corresponding materials of this third class, $[Hf(TPP)]_2[SO_4(H_2O)]_2$ (**7**) and $[Hf(TTP)]_2[\mu\text{-}SO_4(CH_3OH)]_2$ (**8**), is demonstrated in Figure 3. Two sulfate ions are used for the dimer formation to balance the charge, each directing one O-site at each adjacent Hf ion at *ca.* 2.05−2.15 Å. The coordination sphere of the hafnium is supple-

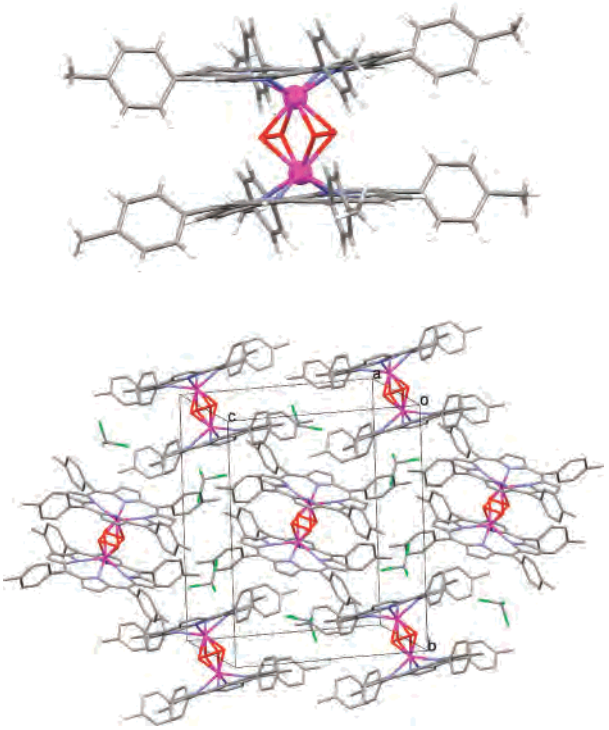

Figure 2. Top: molecular structure of the peroxo-bridged eclipsed dimer $[Hf(TTP)]_2(\mu\text{-}\eta^2\text{-}O_2)_2$ shown with the O−O bonds of the peroxo bridging molecules. The bottom shows the packing in the chloroform solvate. Note the corrugated layers of the metalloporphyrin entities, and the chloroform solvent species intercalated between them. Neighboring layers contain units of the complex oriented in slightly different directions (in a herringbone style) to efficiently accommodate the peripheral methyl groups of the tolyl residues. The analogous phenyl compound $[Hf(TPP)]_2(\mu\text{-}\eta^2\text{-}O_2)_2$ is characterized by similar intercoordination features.

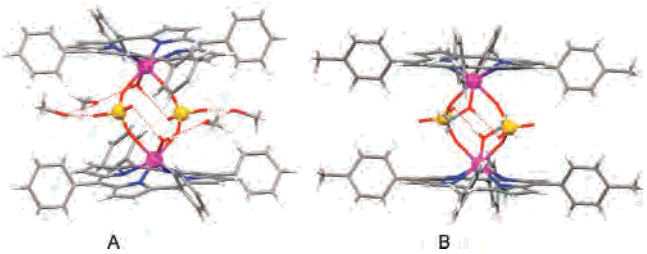

Figure 3. (a) Molecular structure of a $[Hf(TPP)]_2[SO_4(H_2O)]_2$ dimer sustained by two SO_4^{2-} bridges and solvated by four molecules of methanol (compound **7**, Table 3). Note the additional water ligand coordinated to the Hf-ions, and the four molecules of the methanol solvent that interlink by hydrogen-bonding (dotted lines) between the sulfate and water ligands. (b) Molecular structure of $[Hf(TTP)]_2[SO_4(CH_3OH)]_2$ where a molecule of methanol occupies the seventh coordination site.

mented (to CN = 7) by attracting an additional neutral water in the TPP derivative or methanol in the TTP derivative from the crystallization solvent, with a Hf−O(water/methanol) coordinating bond distance of *ca.* 2.25−2.29 Å. In $[Hf(TPP)]_2[SO_4(H_2O)]_2$, the O-sites of the sulfate ions that do not coordinate to Hf are solvated by molecules of methanol via hydrogen bonds (Figure 3a, four methanol molecules per dimer). In $[Hf(TPP)]_2[SO_4(CH_3OH)]_2$, the Hf-coordinated methanol ligand also hydrogen bonds to the adjacent sulfate anion (Figure 3b, Table 5). The larger size of the bridging sulfate ions (as compared to the peroxo bridges discussed above) results in a considerably larger Hf···Hf distance within the dimer (Table 4), but despite the larger size of the

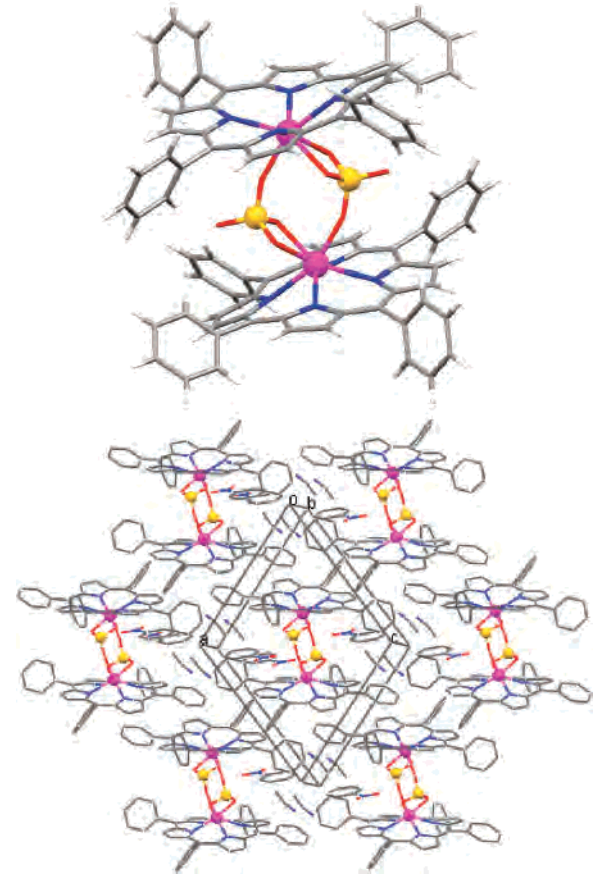

Figure 4. Top: Molecular structure of dimer $[(TPP)Hf(SO_4)]_2$ with the asymmetric coordination of the two SO_4^{2-} bridges to the Hf ions. Bottom: Crystal packing diagram of $[(TPP)Hf(SO_4)]_2$. Note the interstitial occlusion of the nitrobenzene and acetonitrile solvents.

dimeric complex, the crystal-packing modes in the two sulfate-bridged compounds (which crystallized as chloroform solvates) are generally similar to the motif observed in peroxo-bridged examples (see in Supporting Information). Solvent in the interstitial space is ordered in **7** and a disordered **8**.

Another variant of this type of compound is represented by the $[(TPP)Hf(SO_4)]_2$ dimer (**9**), obtained from a nonaqueous environment (nitrobenzene and acetonitrile served as crystallization solvents in this case). Again, two sulfate anions serve as bridges (as well as suitable counterions) between two monomeric $[Hf(TPP)]^{2+}$ entities (Figure 4). However, in the present example these ions serve as the only ligands to the Hf metal (as no other oxo ligands were present in the reaction mixtures). Thus, in order to preserve the seven-coordination environment (as for the other sulfate complexes) two O-atoms of one sulfate and one O-atom of the second sulfate associate with each Hf at 2.08−2.18 Å (Table 4). Slightly longer bonding distances within this range characterize the former, while the latter represents the shortest distance. The crystal packing of $[(TPP)Hf(SO_4)]_2$ is depicted in Figure 4, revealing a layered intermolecular organization similar to previous examples. Molecules of the nitrobenzene and acetonitrile (disordered) solvent are accommodated in the lattice between the metalloporphyrin moieties.

In all three sulfate structures the dimer complexes reside on centers of crystallographic inversion, with identical

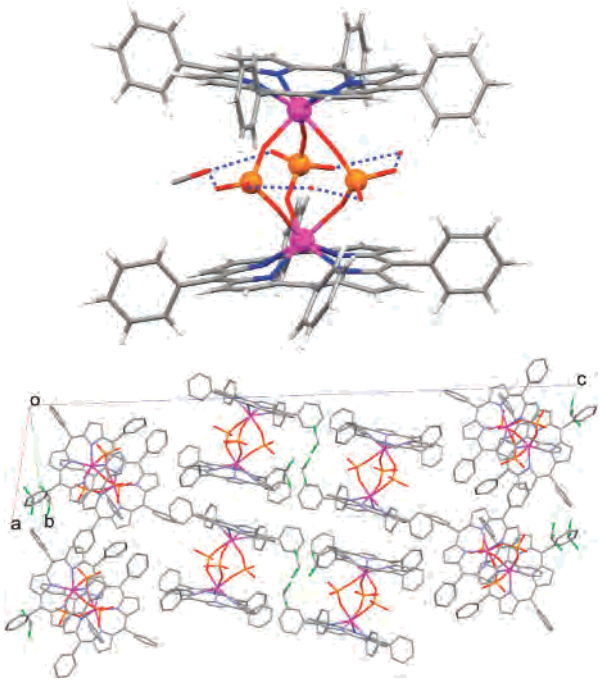

Figure 5. Top: Molecular structure of dimer $[Hf(TPP)]_2(HPO_4)_3^{-2}$, sustained by intercoordination through three (partly disordered) PO_4^{3-} bridges. The latter are further interlinked to one another on the periphery by H-bonds (dotted lines) through MeOH and water species. Bottom: crystal packing diagram of $[Hf(TPP)]_2(HPO_4)_3^{-2}$. Only the chloroform solvent occluded within the bilayers is shown, the additional (partly disordered) water and methanol solvent species being omitted for clarity.

geometries of the two monomeric Hf−TPP constituent parts. Moreover, both the peroxo-bridged and sulfate dimers exhibit an approximate C_{2h} symmetry with the two-fold axis and the pseudomirror plane (the two porphyrin rings assuming an eclipsed orientation) passing through the Hf ions and the median plane of the bridging ligands, respectively.

Although the actual identity of the porphyrin scaffold (whether TPP, TPyP, or TTP) has negligible effect on the molecular structures described above, it does influence to some extent the layered organization of the monomeric or dimeric complexes. The TPP- and TPyP-based compounds organize in space in a parallel fashion, within as well as between the layers. On the other hand, TTP-based materials with a larger molecular framework pack in a herringbone manner, while preserving the layered organization. The molecular units in subsequent layers are slightly tilted with respect to the mean plane of the given layer. This seems to be required by the need to optimize condensed packing of the additional peripheral methyl substituents on the phenyl residues.

Reaction of the Hf−TPP moiety with excess phosphoric acid yields another type of dimer with a different structural motif, $[Hf(TPP)]_2(HPO_4)_3^{2-}$ (**10**), where three phosphate ions serve as bridging units (Figure 5) and hydronium ions are assumed to balance the negative charge of the parent complex. This is the only product in the series of the Hf−porphyrin dimers, which deviates from the axial two-fold symmetry and therefore does not contain an inversion center. The entire dimer represents the asymmetric unit (in which the bridging phosphates suffer from partial disorder) in this structure. The minimal coordination requirements of each Hf ion are satisfied by its bonding to the four pyrrole N-atoms of TPP and the O-atoms of the three tetrahedral phosphate bridges (CN = 7). Noteworthy are the relatively short deviation of the Hf ion from the mean plane of the coordinating O-atoms and the Hf−O distances in this structure (Table 4) due to the stronger electrostatic attraction between the metal and the phosphate ions. In the resulting structure the two/four-fold symmetry of the porphyrin rings is incommensurate with the three-fold symmetry of the bridged Hf-$(PO_4)_3$-Hf fragment. As a result, the fully eclipsed orientation of the porphyrin components of the previous six dimers is not observed. Rather, the two porphyrin macrocycles are partly staggered, which also appears to affect the crystal packing. The outer, noncoordinating O-sites of the phosphate ions are solvated by molecules of water and methanol solvents, each of the latter hydrogen bonding simultaneously to, and interlinking between, two phosphate species (Table 5). The crystal packing of this compound also differs from that observed in the other dimers (Figure 5). Crystal packing consists of bilayers of similarly oriented species and a herringbone organization of these bilayers along the *c*-axis. A considerable amount of partly disordered solvent (CH_2Cl_2, CH_3OH, H_2O, and H_3O^+) is trapped between the metalloporphyrin units in the crystal lattice.

Conclusions

These methods expanded the range of tetraaryl porphyrinates that can be metalated with the Hf(IV) ion. The methods allow access to a plethora of oxygen-bearing ligands by elution from silica using the corresponding acids. Crystallographic studies reveal that despite the diverse array of molecular architectures, the macrocycle distortions and crystal packing are similar. This provides a basis for using these compounds as tectons in the design of solid-state materials with hierarchical supramolecular architectures. The unexpected sulfate- and phosphate-bridged dimeric structures indicate that these multitopic anions may be added to the design palette as components for self-assembly and self-organization of metallocomplexes containing oxophillic metals, such as metalloporphyrin chromophores. The bis-peroxide-bridged complexes result most probably from a redox process with dioxygen and a sacrificial reductant in the crystallization mixture.[16,17] Preliminary work shows that the routes reported herein are applicable to the formation of the Zr(IV) porphyrinates using $Zr(IV)Cl_4$ as a starting material with similar yields.

Acknowledgment. This work was supported by the National Science Foundation (CHE- 0554703 to C.M.D.) and The National Institutes of Health (SCORE S06GM60654 to C.M.D.). A.F. acknowledges support from The National Science Foundation (IGERT DGE-9972892) and an NSF AP Fellowship (DGE-0231800). I.G. acknowledges support from the Israel Science Foundation. Hunter College Chemistry infrastructure is supported by the National Science Foundation, National Institutes of Health, including the RCMI program (G12-RR-03037), and the City University of New

York. We thank Professor Klaus Grohmann for assistance with the diazomethane reactions and Professor Lynn Francesconi for useful discussions.

Supporting Information Available: (1) Further synthetic consideration, including compounds that were not part of the crystallographic studies, (2) UV-visible, ^{1}H NMR, and mass spectrometry data, (3) further crystallographic data and crystallographic information files (CIF). This material is available free of charge via the Internet at http://pubs.acs.org.

IC700840J